



HAL
open science

Observations and Mechanisms for the Formation of Deep Equatorial and Tropical Circulation

Claire Ménesguen, Audrey Delpech, Frédéric Marin, Sophie Cravatte, Richard Schopp, Yves Morel

► **To cite this version:**

Claire Ménesguen, Audrey Delpech, Frédéric Marin, Sophie Cravatte, Richard Schopp, et al.. Observations and Mechanisms for the Formation of Deep Equatorial and Tropical Circulation. *Earth and Space Science*, 2019, 6 (3), pp.370-386. 10.1029/2018EA000438 . hal-02349703

HAL Id: hal-02349703

<https://hal.science/hal-02349703>

Submitted on 5 Nov 2019

HAL is a multi-disciplinary open access archive for the deposit and dissemination of scientific research documents, whether they are published or not. The documents may come from teaching and research institutions in France or abroad, or from public or private research centers.

L'archive ouverte pluridisciplinaire **HAL**, est destinée au dépôt et à la diffusion de documents scientifiques de niveau recherche, publiés ou non, émanant des établissements d'enseignement et de recherche français ou étrangers, des laboratoires publics ou privés.

1 **Observations and mechanisms for the formation of deep**
2 **equatorial and tropical circulation**

3 **Claire Ménesguen¹, Audrey Delpech², Frédéric Marin², Sophie Cravatte²,**
4 **Richard Schopp¹, Yves Morel²**

5 ¹Laboratoire d'Océanographie Physique et Spatiale UMR 6523 CNRS-Ifremer-IRD-UBO, France
6 ²LEGOS, Université de Toulouse, CNES, CNRS, IRD, Toulouse, France

7 **Key Points:**

- 8 — Observation of deep Equatorial and Tropical Circulations : a complex system
9 of zonal jets
10 — Review of theories explaining the generation mechanisms of the Equatorial and
11 Tropical jets
12 — Remaining gaps and future challenges in our global understanding of Deep Equatorial
13 and Tropical Circulations

Corresponding author: Claire Ménesguen, claire.menesguen@ifremer.fr

Abstract

The Intermediate and Deep Equatorial and Tropical Circulations (DEC and DTC) consist of a complex system of zonal jets. This paper attempts at unifying existing observations and theories to present our current understanding of this jets system.

Recent in-situ observations suggesting a continuity between DEC and DTC are confronted against the various generation mechanisms that have been proposed in the literature. The key notion to differentiate these previous studies lies in the so-called "cascade of mechanisms", i.e. the energy pathway and equilibration processes chain that lead to the jets from their initial energy source.

Many studies see the Deep Equatorial Intra-seasonal Variability (DEIV) as the initial energy source, highlighting its key role in energizing the DEC and DTC. However, critical gaps remain in this cascade of mechanisms and limit substantially our ability to represent the jets in Ocean Global Circulation Models. This paper aims at identifying such gaps and propose future research directions.

1 Introduction

Understanding and modeling the intermediate and deep circulation in the equatorial oceans remains one of the great challenge in physical oceanography. For long, observations have shown that the deep equatorial circulation consists in several systems of zonal jets with rather complex features [Luyten and Swallow, 1976; Eriksen, 1981, 1982; Leetmaa and Spain, 1981; Firing, 1987; Ponte and Luyten, 1989, 1990; Firing et al., 1998; Gouriou et al., 1999, 2001; Rowe et al., 2000; Johnson et al., 2002; Dengler and Quadfasel, 2002; Boulès et al., 2003; Ollitrault et al., 2006; Bunge et al., 2008; Ascani et al., 2010, 2015; Brandt et al., 2011; Cravatte et al., 2012; Qiu et al., 2013a; Ollitrault and Colin de Verdière, 2014; Youngs and Johnson, 2015; Cravatte et al., 2017]. However, our current knowledge of the spatial structure and variability of the jets system is far from being comprehensive, and remains an intense subject of investigation. The very existence of these zonal jets has even been questioned by some studies, claiming that the sparse observations only captured aliased planetary waves signals [e.g. Jochum and Malanotte-Rizzoli, 2003]. More recent and comprehensive observational datasets however corroborated the existence of mean zonal currents, on which seasonal Rossby waves currents superimpose. They suggest that the near-equatorial zonal currents should not be considered as isolated pieces [Cravatte et al., 2012, 2017], but rather appear as embedded into a broader meridional system of zonal jets extending to the tropics.

These new observations challenge the many studies that have attempted a theoretical explanation of the presence of the jets in the equatorial region [Marin et al., 2000; Jochum and Malanotte-Rizzoli, 2004; d'Orgeville et al., 2007; Hua et al., 2008; Ménesguen et al., 2009a; Fruman et al., 2009; Ascani et al., 2010, 2015] and further away in the tropics [Marin et al., 2000; Jochum and Malanotte-Rizzoli, 2004; d'Orgeville et al., 2007; Hua et al., 2008; Ménesguen et al., 2009a; Fruman et al., 2009; Ascani et al., 2010, 2015]. None of them has succeeded in explaining the whole currents system observed from direct measurements highlighting the lack of comprehensive theoretical understanding of Deep Equatorial and Tropical Circulations (DEC and DTC).

This paper is an effort to review our current knowledge of the equatorial and tropical dynamics from subsurface to depth. Its goal is to revisit the existing theories of the mechanisms leading to the Deep Equatorial Circulation (DEC) and Deep Tropical Circulation (DTC) formation, in the light of recent observations. It does not pretend to provide a comprehensive analysis of all the theoretical and modeling studies on zonal jets formation. Rather, it aims to discuss mechanisms specifically relevant for DEC formation, and their possible extension to DTC formation. Indeed, as a tribute to the memory of Lien Hua, we focus on Hua et al. [2008]'s theory, and the mechanisms they proposed.

64 We show that other theories on DEC share a common interpretation of the formation
 65 of jets as the results of a cascade of mechanisms. We will also address the question of
 66 the applicability of this theory and approach to a broader latitudinal range.

67 The paper first summarizes, in section 2, the observations of the main features of
 68 DEC and DTC, interpreted as a general system of zonal jets. It then discusses, in sec-
 69 tion 3, the existing theories for the formation of zonal jets, described as a cascade of me-
 70 chanisms involving key energy sources from which the energy is extracted, and equili-
 71 bration processes, explaining the formation of stable basin-scale jet structures. In the last
 72 section, a discussion on the importance of the key energy sources, focused on the Deep
 73 Equatorial Intra-seasonal Variability (DEIV), for the DEC and DTC characteristics is
 74 proposed, with open questions toward a possible unifying theory. Gaps in our current
 75 knowledge and needs for future model developments to better understand the equator-
 76 ial and low-latitudes system are also discussed.

77 2 Observations of the Deep Equatorial and Tropical Circulation (DEC 78 and DTC)

79 One striking characteristic of the tropical oceans is the complex set of zonal cur-
 80 rents observed at intermediate and deeper depths (500-2000m) over the whole basin. Cross-
 81 equatorial surveys revealed the presence of two patterns of alternating eastward and west-
 82 ward jets schematically represented in Figure 1 : (1) the Equatorial Deep Jets (EDJs),
 83 which are equatorially-trapped, vertically-alternating zonal currents with a vertical scale
 84 of a few hundreds of meters ; (2) the Extra-Equatorial jets (EEJ) or Equatorial Inter-
 85 mediate Currents (EICs), which are a series of latitudinally-alternating zonal currents
 86 with a large vertical extent, and a meridional wavelength of about 3° . This section de-
 87 scribes the characteristics of these zonal current systems, their persistence, as well as their
 88 similarities and differences in the different basins. Main abbreviations of the different de-
 89 signations of zonal jets are summarized in Table 1 and their main characteristics are gi-
 90 ven in Table 2.

91 2.1 Characteristics of the Zonal Equatorial Deep Jets (EDJs)

92 EDJs are equatorially-trapped (1.5°N - 1.5°S) eastward and westward jets stacked
 93 over the vertical, with typical wavelengths between 300 and 700 meters [*Youngs and John-*
 94 *son, 2015*]. They are ubiquitous below the thermocline, extend basin-wide, and are vi-
 95 sible in instantaneous profiles, suggesting that they are permanent features of the cir-
 96 culation. They have been observed in all three equatorial basins, though with different
 97 properties ; in the Pacific [*Eriksen, 1981; Leetmaa and Spain, 1981; Firing, 1987; Ponte*
 98 *and Luyten, 1989; Johnson et al., 2002*], in the Atlantic [*Eriksen, 1982; Gouriou et al.,*
 99 *1999, 2001; Boulès et al., 2003*] and in the Indian Oceans [*Luyten and Swallow, 1976;*
 100 *Ponte and Luyten, 1990; Dengler and Quadfasel, 2002*]. In the Pacific Ocean, they ap-
 101 pear to be weaker (10 cm/s) and exhibit a smaller vertical wavelength (300-400 m) than
 102 in the Atlantic Ocean (20 cm/s, 500-700m) or the Indian Ocean (15-20 cm/s, 300-600m).

103 The EDJs zonal continuity, persistence and vertical migrations have been the sub-
 104 ject of debate, because of the difficulty to characterize them with sparse data. Multi-years
 105 of moored velocity observations and large-scale hydrological profiles showed that EDJs
 106 exhibit a slow downward phase propagation (and associated upward energy propagation
 107 in the framework of linear wave theory), implying the existence of an energy source at
 108 depth, over a 12-30 years period in the Pacific Ocean [*Johnson et al., 2002; Youngs and*
 109 *Johnson, 2015*], and a period of around 4.5 years in the Atlantic Ocean [*Johnson and*
 110 *Zhang, 2003; Bunge et al., 2008; Brandt et al., 2011; Claus et al., 2016*] and in the In-
 111 dian Ocean [*Youngs and Johnson, 2015*].

112 2.2 Characteristics of the Extra-Equatorial Jets (EEJs)

113 The extra-equatorial jets are a system of meridionally-alternating westward and
 114 eastward jets, with a large vertical extent, and a 3° meridional wavelength. They are ob-
 115 served at intermediate depths (500-1500m) in both the Atlantic and Pacific Oceans. No
 116 evidence of such zonal current systems has been provided yet in the Indian Ocean.

117 Our knowledge of these zonal jets first came from synoptic cross-equatorial sections ;
 118 they were first thought to be confined to the near-equatorial 3°S - 3°N band [*Firing*, 1987],
 119 with a striking zonal coherence across the Pacific basin [*Firing et al.*, 1998]. In this la-
 120 titudinal band, this system is composed of the eastward North and South Intermediate
 121 Countercurrents (NICC and SICC) located at 1.5° - 2° , and the westward North and South
 122 Equatorial Intermediate Currents (NEIC and SEIC) found at 3° [*Ascani et al.*, 2010].
 123 Extended meridional sections revealed that similar westward and eastward jets are also
 124 present further off-equator [e.g. *Gouriou et al.*, 2006; *Qiu et al.*, 2013a].

125 The advent of the Argo program allowed estimations of 10-day mean velocity at
 126 the floats' parking depth and provided the first basin-wide pictures of zonal currents at
 127 1000m depth in the Atlantic and Pacific Oceans [*Ollitrault et al.*, 2006; *Ascani et al.*, 2010,
 128 2015; *Cravatte et al.*, 2012, 2017; *Ollitrault and Colin de Verdière*, 2014]. These studies
 129 confirmed that alternating zonal jets extend in the tropics to at least 18° , with a remar-
 130 kable zonal coherence in the basin at this depth, and suggested that the NICC, SICC,
 131 NEIC and SEIC may be part of a much broader meridionally-alternating current sys-
 132 tem. In the Pacific and Atlantic, these jets have mean velocities of about 5 to 10 cm/s
 133 but instantaneous estimations are much larger (see *Cravatte et al.* [2017]). They are stron-
 134 ger in the Southern Hemisphere, stronger in the western part of the basin, and weaken
 135 and disappear toward the eastern part of the basin [*Cravatte et al.*, 2012].

136 Recently, *Cravatte et al.* [2017] investigated the vertical structure of these EEJs in
 137 the Pacific Ocean with a combination of direct velocity measurements and geostrophic
 138 estimations. They found a complex vertical structure, consisting in two apparently dis-
 139 tinct systems of meridionally-alternating zonal jets equatorward of 10° (Figure 1 ; see
 140 *Cravatte et al.* [2017] and Table 1 for the terminology) :

- 141 – above 800m, the Low Latitude Subsurface Countercurrents (LLSCs) including the Tsu-
 142 chiya jets [*Rowe et al.*, 2000], are found just below the thermocline and feel its large-scale
 143 slope. These jets deepen and get denser poleward ; they also shoal to lighter density and
 144 shift poleward from west to east, thus exhibiting a variable meridional wavelength [*Cra-*
 145 *vatte et al.*, 2017]. Their mean amplitude of about 20 cm/s or greater close to the equa-
 146 tor, weakens to 5 cm/s further poleward.
- 147 – below 800m, the Low Latitude Intermediate Currents (LLICs) (including the SICC,
 148 NICC, NEIC and SEIC) seem to be a different system of meridionally-alternating zo-
 149 nal jets with a smaller wavelength (3° , Table 2), found on a large vertical extension down
 150 to 2000m. Unlike the LLSCs, the latitudinal positions of the LLICs remain constant throu-
 151 ghout the basin [*Cravatte et al.*, 2012, 2017].

152 Both systems of currents merge and are indistinguishable poleward of 10° .

153 Excepting the Tsuchiya jets which are permanent features of the circulation, the
 154 EEJs amplitude and position vary from one instantaneous section to another [e.g. *Gou-*
 155 *riou et al.*, 2006; *Cravatte et al.*, 2017]. This is partly explained in the near-equatorial
 156 band by the seasonal variability of the currents, related to vertically-propagating annual
 157 Rossby waves [*Marin et al.*, 2010]. As the seasonal zonal current anomalies are of simi-
 158 lar amplitude or larger than the mean currents on which they superimpose, EEJs may
 159 disappear or reverse direction from one section to another. Variability at intra-seasonal
 160 and interannual timescales is also observed [*Firing et al.*, 1998; *Cravatte et al.*, 2017], though
 161 largely unexplored. These jets and their zonal continuity is thus better revealed on aver-
 162 aged sections, raising the question of the nature of these jets and whether they are la-
 163 tent or permanent features of the circulation. Thus their transport properties have to

164 be assessed. At least, the comparison of 1000m-depth velocities from Argo floats displa-
 165 cements averaged over different periods of 4 years covering the Argo era give similar am-
 166 plitudes and positions for the LLICs (not shown). This suggests that the LLICs inter-
 167 annual variability, if any, is at periods longer than the Argo era (15 years); this also sug-
 168 gests that LLICs are not the result of averaging randomly distributed eddies.

169 **3 Review of proposed mechanisms for the formation and equilibration** 170 **of the DEC and DTC**

171 **3.1 A cascade of mechanisms**

172 Recently, different theories have been proposed to explain some elements of the sys-
 173 tem of zonal jets described in Figure 1. As in *Hua et al.* [2008] these theories involve a
 174 cascade of mechanisms transferring energy from an initial source to equilibrated zonal
 175 jet structure. In this cascade of mechanisms, the main ingredients that we can identify
 176 are : a key energy source, transfer processes and equilibration processes.

177 This cascade of mechanisms is schematically represented in Figure 2. Three main
 178 energy sources have been proposed in the literature for the generation of various parts
 179 of the tropical system of zonal jets :

- 180 – the Deep Equatorial Intra-seasonal Variability (DEIV) : originating either from the
 181 wind, the instability of deep western boundary currents or from Tropical Instability Waves
 182 (that are triggered by the instability of near-surface currents and then partly propagate
 183 their energy to depth), this energy source have been invoked for the generation of EDJs
 184 and the surrounding SICC and NICC [e.g. *Hua et al.*, 2008; *Ascani et al.*, 2015] or for
 185 the observation of Tsuchiya Jets in *Jochum and Malanotte-Rizzoli* [2004].
- 186 – Extra-equatorial annual Rossby waves : forced by the seasonal variations of winds, they
 187 can lead to the formation of the extra-equatorial zonal jets at latitudes where the LLSC
 188 and LLIC have merged (typically poleward of 10°) [e.g. *Qiu et al.*, 2013b].
- 189 – Regional permanent features of the ocean circulation or of the wind forcing : upwel-
 190 lings or the equatorial shoaling of the thermocline can explain the formation of the first
 191 SSCCs (or Tsuchiya jets) below the thermocline ; small meridional-scale structure of the
 192 wind stress curl has also been proposed away from the equator [e.g. *Marin et al.*, 2003;
 193 *Taguchi et al.*, 2012].

194 These different energy sources thus apply to different regions of the equatorial or
 195 tropical ocean. The two first energy sources are associated with time-variable forcings
 196 (intra-seasonal or seasonal waves), whereas the last one can be mainly seen as a response
 197 to permanent ocean or atmosphere forcing. These energy sources are prone to instabi-
 198 lities and mixing, that convert initial energy to other scales. Finally, equilibration me-
 199 chanisms, involving turbulent processes (e.g. nonlinear rectification) or waves interac-
 200 tions (e.g. basin adjustment or modes, secondary instabilities such as inertial or para-
 201 metric instabilities), lead to the final formation of the zonal jets (cf Figure 2).

202 As discussed below, if DEIV is thought to be the main mechanism for the forma-
 203 tion of the vertically-alternating EDJs, there is not a unique key forcing for the system
 204 of meridionally-alternating zonal jets. Different mechanisms are invoked for various ele-
 205 ments of this system, and some have no theory to explain their formation. Because all
 206 jets belong to an apparently organized system, we discuss their generation mechanisms
 207 following a common formalism. Therefore the following sections follow the schematic dia-
 208 gram of Figure 2 and discuss first the different key energy sources and the associated energy
 209 transfer processes, and then the equilibration processes of the zonal jets.

210 **3.2 Key energy sources and energy transfer processes toward zonal jets**
 211 **formation**

212 **3.2.1 The Deep Equatorial Intraseasonal Variability (DEIV) and the**
 213 **DEC formation**

214 Most recent studies [*Hua et al.*, 2008; *d’Orgeville et al.*, 2007; *Ménesguen et al.*, 2009a;
 215 *Fruman et al.*, 2009; *Ascani et al.*, 2010, 2015] have identified the Deep Equatorial In-
 216 traseasonal Variability (DEIV) as the main source of energy for the generation of per-
 217 manent zonal jets in the vicinity of the equator (red boxes in Figure 2). The DEIV is as-
 218 sociated with an equatorial Mixed Rossby-Gravity wave (so-called MRG or Yanai wave)
 219 with different characteristics. Figure 4 illustrates in a non-dimensional diagram the wa-
 220 venumber of MRG waves characteristics for some studies. *Ménesguen et al.* [2009a] or
 221 *d’Orgeville et al.* [2007] used short waves as primary energy sources (and long waves were
 222 stable in their simulations), while *Ascani et al.* [2015] and specially *Ascani et al.* [2010]
 223 considered longer waves that are more divergent and further away from short Rossby waves
 224 characteristics. Different processes have thus been invoked for extracting energy from the
 225 primary waves.

226 *Hua et al.* [2008]; *d’Orgeville et al.* [2007]; *Ménesguen et al.* [2009a]; *Fruman et al.*
 227 [2009] considered energy transfers when primary MRG waves are unstable, transferring
 228 their energy to smaller scales. Their theory comes from *Lorenz* [1972]’s and *Gill* [1974]’s
 229 theory who have studied, in a 2D β -plane configuration, the destabilization of Rossby
 230 waves. *Gill* [1974] showed that Rossby waves are always unstable. The destabilization
 231 process is a function of the wave intensity, measured by the adimensional number $M =$
 232 Uk^2/β , where U is the maximum current of the wave, k is its wavenumber and β the pla-
 233 netary vorticity gradient. Strong waves (moderate to large M) are subject to barotro-
 234 pic instability, weaker waves (small M) to triadic instabilities. In both cases, the growth
 235 rate of the most unstable mode is proportional to Uk . For strong waves, the most unsta-
 236 ble mode has a wavenumber perpendicular to the one of the primary wave with a wa-
 237 velength of the order of $1/k$. It means that a short zonally-sheared wave will be desta-
 238 bilized into zonal jet-like structures. In the equatorial region, this study has been adap-
 239 ted by *Hua et al.* [2008] to the destabilization, in a stratified ocean, of short equatorial
 240 MRG waves (which have characteristics similar to short Rossby waves). Thus, *Hua et al.*
 241 [2008] showed that short equatorial MRG waves are destabilized into zonal currents with
 242 a meridional scale similar to the (short) zonal wavelength of the primary wave, indepen-
 243 dently from the primary wave’s vertical structure. Because, in the equatorial region, the
 244 vertical scale of the baroclinic waves is tied to their meridional scale through the equa-
 245 torial radius of deformation, short meridional scale is reached through either high me-
 246 ridional wavenumber, either high vertical modes. Thus, the specificity of the equatorial
 247 region is that the destabilization of a MRG wave produces both EDJ- and EEJ-like struc-
 248 tures : the emerging EDJs are identified as a high baroclinic basin modes (a combina-
 249 tion of long Kelvin and Rossby waves) and its vertical scale is proportional to the square
 250 of the zonal wavelength of the primary wave, while the emerging EEJs are identified as
 251 a low baroclinic basin modes, but with high meridional wavenumber.

252 In an idealized basin configuration, *Ascani et al.* [2015] [see also *Matthießen et al.*,
 253 2017] have imposed DEIV and achieved an equilibrated simulation reproducing main fea-
 254 tures of the DEC, like EDJs and EEJs. They analyzed energy transfers between waves
 255 and they confirmed that MRG waves (from 30- to 100 day period) participate in the ge-
 256 neration of EDJs. They also evidenced energy transfers from short Rossby waves (with
 257 periods between 50 and 100 days and large vertical scale) to the EEJ. This is in agree-
 258 ment with *Hua et al.* [2008], but more unexpectedly, they also evidenced a more com-
 259 plex energy transfer from EDJ basin modes to the EEJs.

260 **3.2.2 The extra-equatorial annual Rossby waves and the DTC forma-** 261 **tion**

262 Focusing on the generation of three subthermocline eastward jets between 9°N and
 263 18°N below the thermocline in the northern Tropical Pacific, *Qiu et al.* [2013b] propose
 264 annual Rossby waves as a key energy source (blue boxes in Figures 2). Because of their
 265 different characteristics in comparison with DEIV, the processes involved in the energy
 266 transfer and equilibration to jets are different from what we discussed above. From both
 267 theoretical considerations and numerical models, they conclude that these low baroclinic
 268 zonal jets result from two successive processes : (i) the generation of meso-scale eddies
 269 through the instability, by wave-triad interactions, of wind-forced annual first-baroclinic
 270 Rossby waves in the eastern Pacific and (ii) the subsequent formation of zonal jets through
 271 the convergence of potential vorticity (PV) fluxes associated with the eddies. In this fra-
 272 mework, the jets appear as latent jets (following the denomination proposed by *Berloff*
 273 *et al.* [2011]), i.e. as weak jets relative to ambient eddies, for which long-term time ave-
 274 rages are needed to isolate them.

275 **3.2.3 Permanent forcings for subthermocline DTC formation**

276 The Tsuchiya jets (or primary SCCs as contoured in green in the schematic dia-
 277 gram of Figure 2) were the first observed jet structures off the Equator. Early studies
 278 have been argued that they simply result from permanent regional oceanic or atmosphe-
 279 ric forcings. Besides TIWs [*Jochum and Malanotte-Rizzoli*, 2004], three permanent energy
 280 sources have been proposed to explain the creation of the Tsuchiya jets :

- 281 – The Equatorial UnderCurrent (EUC) : *McPhaden* [1984] was the first to analyse the
 282 dynamics associated with the Tsuchiya jets, seen as lobes of the EUC on both sides of
 283 the equator, resulting from a balance between the poleward diffusion of the cyclonic vor-
 284 ticity associated with the EUC, and the poleward advection of planetary vorticity. Such
 285 a balance can only hold in the westernmost part of the equatorial Pacific, and other pro-
 286 cesses (such as nonlinearities) are required to explain the poleward shift of the Tsuchiya
 287 jets (and their progressive separation from the EUC) from West to East.
- 288 – The eastern boundary upwelling system : From both analytic and numerical layered
 289 models of the tropical Pacific, *McCreary et al.* [2002] suggest that the Tsuchiya jets are
 290 mostly driven by upwelling along the South America coast and in the Costa-Rica Dome
 291 below the InterTropical Convergence Zone (ITCZ). The Tsuchiya jets are explained as
 292 geostrophic currents along arrested fronts, generated by the convergence or intersection
 293 of the characteristics of the Rossby waves carrying information about the density struc-
 294 ture away from the upwelling regions. Diapycnal fluxes between layers, and the presence
 295 of a prescribed Pacific inter-ocean circulation (representing the Indonesian throughflow
 296 and a compensating inflow at greater depths from the South), are necessary to create
 297 the jets. These results have been further supported in global and regional OGCMs for-
 298 ced by idealized winds [*Furue et al.*, 2007, 2009].
- 299 – The equatorward shoaling of the thermocline : *Marin et al.* [2000] propose a mecha-
 300 nism similar to the atmospheric Hadley cells to explain the Tsuchiya jets. In response
 301 to the large-scale equatorial shoaling of the ventilated thermocline, meridional ageostro-
 302 phic and diapycnal cells are created and redistribute angular momentum, creating east-
 303 ward jets analogue to the atmospheric Jet Streams. In their two-dimensional model, the
 304 meridional structure of the thermocline is prescribed and diapycnal fluxes result from
 305 an ad hoc relaxation to this background density field. In subsequent papers, *Hua et al.*
 306 [2003] and *Marin et al.* [2003] show that this mechanism still holds for a fully three-dimensional
 307 Primitive Equations model where the ventilated thermocline is forced by basin-scale Ek-
 308 man pumping, with strong equatorial recirculations.

309 The small-scale structure of wind stress curl has also been proposed as a mecha-
 310 nism for the formation of zonal jets below the thermocline, in the presence of islands or
 311 in the Southern Pacific Ocean. The local wind stress curl anomalies generated in the lee

312 of an island has been recognized as a forcing for zonal circulation west of this island [e.g.
 313 *Belmadani et al.*, 2013]. Following *Kessler and Gourdeau* [2006], *Taguchi et al.* [2012] sug-
 314 gest that the deep oceanic zonal jets observed in the southern tropical ocean are partly
 315 forced by coupled ocean/atmosphere processes. In their coupled general circulation model,
 316 the deep zonal jets have a signature at the surface, inducing Sea Surface Temperature
 317 (SST) anomalies at the same spatial scales through zonal advection. These SST ano-
 318 malies impact the atmosphere, creating small-scale wind stress curls collocated with the
 319 temperature anomalies, which reinforce the zonal jets in accordance with Sverdrup ba-
 320 lance.

321 If these different theories can associate subthermocline zonal jets structure to large-
 322 scale or regional permanent forcings, they however can not explain deeper zonal jets. These
 323 theories are not incompatible and it is probable that a combination of the different energy
 324 transfer processes, involving different key energy sources, are taking place in the equa-
 325 torial and tropical regions.

326 3.3 Equilibration processes

327 After the transfer of energy from key sources to new spatial and temporal scales
 328 in equatorial and tropical areas, equilibration processes thus have to take place to form
 329 DEC and DTC (cf Figure 2).

330 3.3.1 DEC equilibration

331 The equilibration mechanism associated with the equatorial wave instabilities pro-
 332 posed in *Hua et al.* [2008] is a direct structuring of the instability of short MRG waves
 333 into zonal currents. The zonal location, the meridional extension of the initial wave, or
 334 the presence of boundaries does not modify the tendency to zonal structuring of the re-
 335 sulting circulation but has an influence on the zonal extension of the jets. It has been
 336 shown that the MRG wave destabilization produces long high baroclinic Kelvin waves
 337 (EDJs-like structures) propagating eastward and long low baroclinic Rossby waves (LLICs-
 338 like structures) propagating westward [*Hua et al.*, 2008; *d’Orgeville et al.*, 2007; *Ménes-
 339 guen et al.*, 2009a; *Fruman et al.*, 2009].

340 – Inertial instability : short time scale equilibration

341 This process has been shown to explain the fast homogenization of PV to zero in-
 342 side the westward jets of the EDJs, while PV exhibits strong gradients on their rim [*Mé-
 343 nesguen et al.*, 2009b]. Since the Coriolis parameter changes its sign at the equator, the
 344 equatorial band is particularly propitious to inertial instability [*Hua et al.*, 1997; *d’Or-
 345 geville and Hua*, 2005; *Fruman et al.*, 2009]. Inertial instability has only been invoked
 346 as a secondary instability and is not necessary to explain the extraction of energy and
 347 the equilibration into zonal jets but it influences the final structure of the EDJ.

348 – Influence of basin modes : long time scale equilibration

349 As discussed in *Matthießen et al.* [2017], eastern and western boundaries have a strong
 350 influence on the equilibration of the zonal jets. In a basin configuration, East and West
 351 walls generate reflexion of equatorial waves. The combination of Kelvin waves and their
 352 reflection into a first meridional-mode long Rossby wave create a basin mode with a per-
 353 iod $T_n = 4L_B/c_n$, with L_B the basin length and c_n the gravity phase speed of the ba-
 354 roclincic mode n . The periodicity for this basin mode is about 4.5 years in the Atlantic
 355 for the vertical mode observed for the EDJs [*Johnson and Zhang*, 2003] and about 12-
 356 30 years in the Pacific [*Youngs and Johnson*, 2015], with a great uncertainty due to wea-
 357 ker amplitude of EDJs and a broader bandwidth for their vertical mode in the Pacific.

358 Most of the studies analyzing the influence of basin mode on the structuring -and
 359 slow variability- of the DEC concerned EDJ. *d'Orgeville et al.* [2007] have highlighted
 360 such low-period oscillations in their simulated solutions of the EDJ. However, they used
 361 an idealized forcing over the whole depth which inhibited the upward energy propaga-
 362 tion and the vertical dissymmetry observed in the ocean. Longer simulations were per-
 363 formed by *Ascani et al.* [2015] and *Matthießben et al.* [2015, 2017] and their use of a sur-
 364 face intensified forcing term lead to more realistic upward energy propagation for the ba-
 365 sin modes, which is however not fully understood. Indeed, in their very long simulations
 366 (over 200yrs), *Matthießben et al.* [2017] have in fact found an alternance of downward and
 367 upward propagating phase of the basin mode. Observations are not long enough to va-
 368 lidate or unvalidate their results and the consequence of the surface-intensified forcing
 369 rather than a forcing at depth on the basin mode energy propagation is thus still an open
 370 question.

371 To our knowledge, few studies have analyzed the effect of boundaries and basin modes
 372 on the structuring of the LLSC or LLIC. Argo available data do not cover a long enough
 373 time period to conclude. A noticeable exception is *Qiu et al.* [2013b]. Even though this
 374 is not clearly stated in their paper, their Figure 3 clearly exhibits a slow meridional pro-
 375 pagation of the low latitude jets structure (with a time period of 50 years or so that is
 376 not discussed). This could be the propagating signature of high meridional basin modes,
 377 that could thus be involved in the formation of the whole EEJ structure, at least in nu-
 378 merical simulations.

379 **3.3.2 Nonlinear rectification**

380 Non-linear rectification can reinforce preexisting jets and contribute to their equi-
 381 libration into permanent circulation features. The influence of eddies through the conver-
 382 gence of PV fluxes is invoked by *Qiu et al.* [2013b] to explain the existence of the low
 383 latitude jets. A similar mechanism was found in the tropical Pacific by *Ishida et al.* [2005],
 384 where high mesoscale eddy activity is shown to accelerate the SCC (especially for the
 385 northern Tsuchiya Jet in the eastern part of basin) and to generate large region of PV
 386 homogenization in which strong horizontal recirculations take place.

387 Besides the permanent forcings that are proposed to explain the Tsuchiya Jets, Tro-
 388 pical Instability Waves have been shown to be an additional contributor to the genera-
 389 tion of the Tsuchiya Jets. Using the Transformed Eulerian Mean equations to explore
 390 the momentum balance of the southern Tsuchiya Jet in a numerical simulation of the
 391 Tropical Atlantic, *Jochum and Malanotte-Rizzoli* [2004] shows that the jet is maintai-
 392 ned against dissipation by the convergence of the Eliassen-Palm flux associated with the
 393 TIW. The TIWs are also seen as an additional driver for the northern Tsuchiya Jet in
 394 *McCreary et al.* [2002], *Hua et al.* [2003] or *Furue et al.* [2009].

395 The convergence of PV or Eliassen-Palm fluxes invoked by these studies is asso-
 396 ciated with the tendency of eddies to reinforce the jets. Indeed, zonal jets are associa-
 397 ted with zonal PV structures which act as a vortex guide, keeping eddies within some
 398 latitudinal bands. Eddies have the tendency to homogenize PV within their vicinity. The
 399 combination of both effects leads to a sharpening of the initial PV structure, with ho-
 400 mogeneous PV region separated by sharp PV gradients, eventually leading to a stair-
 401 case structure. In this case, the characteristics of the eddies determine the final structure
 402 and the width of the jets [*Dritschel and McIntyre*, 2008; *Dritschel and Scott*, 2011; *Scott*
 403 *and Dritschel*, 2012].

404 Besides the equilibration mechanisms reviewed in this section, many other parti-
 405 cularities of the ocean may influence the shape of the jets and explain the features we
 406 observe [e.g. the large scale zonal slope of the thermocline *Johnson and Moore*, 1997].

407 4 Discussion

408 DEIV has thus been invoked in many studies as the key energy source, mainly for
 409 the formation of DEC but also possibly of DTC. As discussed above, there is no consen-
 410 sus on the details of the transfer and equilibration processes, from DEIV to zonal jets,
 411 which depends on the DEIV structure, location and amplitude.

412 In the following sections, we therefore address questions concerning DEIV charac-
 413 teristics in previous studies, focusing on their differences, and in observations.

414 4.1 Influence of the DEIV location on the resulting DEC

415 As recalled before, in *Hua et al.* [2008], MRG destabilization in the equatorial rail
 416 will produce high baroclinic Kelvin waves propagating eastward and low baroclinic Rossby
 417 waves propagating westward. In this linear phase, the location of the destabilization is
 418 thus important for the extent of the zonal jets, specially in a basin configuration. *Hua*
 419 *et al.* [2008] used an artificial analytical deep forcing to create the primary MRG wave
 420 in a channel and in a basin configuration. *d’Orgeville et al.* [2007] and *Ménesguen et al.*
 421 [2009a] have used a similar analytical deep forcing restricted to the western boundary
 422 of an idealized Atlantic basin, mimicking the deep western boundary variability. In every
 423 cases, resulting zonal jets are propagating from the area where the primary wave is des-
 424 tabilized. In basin cases, some energy is lost at eastern or western boundaries. There-
 425 fore, the location of the source of the short MRG wave (propagating eastward) in the
 426 western boundary is important, principally for EEJ that are propagating west of the des-
 427 tabilization zone.

428 *Ascani et al.* [2010] focused on the Pacific basin with the forcing of a vertically pro-
 429 pagating MRG wave excited at surface in a restricted equatorial band. They reprodu-
 430 ced EEJ structures within and west of the forcing area with an amplitude that remains
 431 modest west of the forcing area. In their following study [*Ascani et al.*, 2015], DEIV is
 432 still associated with tropical instability waves transferring the surface variability to the
 433 deeper ocean. Their idealized configuration of an Atlantic basin reproduces a DEC with
 434 EDJ and EEJ like structures in a 6-month mean field. They have noted that the strength
 435 of the EEJ rapidly diminishes away from the western boundary and remains weak if rea-
 436 listic coastlines are used.

437 To summarize, DEIV directly forced at depth or propagating from the surface pro-
 438 duce deep jets structures. In a basin configuration, the horizontal location has an im-
 439 pact on the zonal extension of resulting jets and vertical location an impact on the ver-
 440 tical propagation (as discussed in section 3.3.1).

441 4.2 Influence of the DEIV amplitude and frequency on the resulting DEC 442 and DTC

443 To be able to differentiate the dynamical regimes applied in previous studies and
 444 characteristics of the MRG waves representing DEIV in previous studies, using the vor-
 445 ticity and divergence equations, we derive the general equation governing the dynamics
 446 of these waves, including their forcing. As shown in appendix A: , for trapped equato-
 447 rial waves this equation is :

$$\begin{aligned}
 & \frac{c^3}{c_G^2 c_{sR}} \delta_{xtt} \quad + \frac{c}{c_G} \delta_x \quad + v_x \quad + \frac{c}{c_{sR}} \nabla^2 \frac{P_{xt}}{\rho_0} \quad + M^* [(\mathbf{u} \cdot \nabla \zeta)_x + ONLT] \quad = O(M^{*2}) \\
 & \text{I} \qquad \qquad \text{II} \qquad \qquad \text{III} \qquad \qquad \text{IV} \qquad \qquad \text{V}
 \end{aligned} \tag{1}$$

448 where P is the pressure, $\mathbf{u} = (u, v)$ is the horizontal velocity field, $\delta = \partial_x u +$
 449 $\partial_y v$ is the horizontal divergence, $\zeta = \partial_x v - \partial_y u$ the vorticity and $ONLT$ stands for

450 'other nonlinear terms' whose form is not important for the discussion. The other fac-
 451 tors are scaling characteristics associated with the wave types and are explained in ap-
 452 pendix A: . The terms (I,II,III,IV) are the classical linear part leading to MRG wave while
 453 (V) is the nonlinear term responsible for triadic resonance and barotropic instabilities
 454 leading to turbulence and jets. Table 3 gives their order of magnitude for selected pre-
 455 vious studies involving DEIV :

456 – The scaling shows that *Ascani et al.* [2010] force the equatorial ocean more linearly :
 457 the nonlinear term is smaller than the linear ones, favoring the gravity part of the MRG
 458 wave and departing from the barotropic-like instability (in accordance with Figure 4).
 459 Diabatic processes (vertical mixing) thus has to be invoked to transfer energy from this
 460 type of waves.

461 – At higher latitudes, *Qiu et al.* [2013b] force their simulations with $M^* \ll 1$ which,
 462 following *Gill* [1974]'s theory, is a regime of triadic instabilities, as interpreted by the au-
 463 thors.

464 The length scale needed to destabilize the forced equatorial MRG wave is given by
 465 $L_{dest} \simeq 25 \frac{cY}{kFr_{H_{ua}}}$ [see appendix A: and *Ménesguen et al.*, 2009a]. It is evaluated for
 466 the forcing used the different authors in Table 3. For *Qiu et al.* [2013b], we replaced the
 467 MRG wave speed by the long Rossby wave speed. When the destabilization length scale
 468 is small compared to basin widths, the models have enough time to develop jets (as it
 469 is the case for most of the cases of the table 3). But, we confirmed also that the wave
 470 forced by *Ascani et al.* [2010] is very stable compared to other studies sampled here.

471 4.3 DEIV observations

472 The deep intraseasonal variability can be estimated thanks to the Argo floats, which
 473 drift at 1000-m depth during approximately 9 days between two vertical profiles. Ave-
 474 raging drift velocities from thousands of floats has yielded regional and global maps of
 475 1000-m mean velocity [e.g. *Cravatte et al.*, 2012; *Ollivraut and Rannou*, 2013]. Avera-
 476 ging the anomalous drift velocities can provide estimates of eddy kinetic energy (EKE)
 477 at 1000m [*Ascani et al.*, 2015].

478 Here, we compute for each float dive the 10-day mean lagrangian drift velocity ano-
 479 maly relative to the mean seasonal velocity at the same month and location, and com-
 480 pute for each float dive the 'v-EKE' from the square of the meridional component ano-
 481 maly only. We then map these EKE values with an optimal interpolation method to ob-
 482 tain an estimate of the deep intraseasonal variability (Figure 3). *Bunge et al.* [2008] found
 483 in moored observations that the meridional velocity component at depth in the Atlan-
 484 tic Ocean is dominated by fluctuations at 20-45 days, but that a substantial fraction lies
 485 between 10 and 20 days. *Ogata et al.* [2008] also found variability in the deep meridio-
 486 nal velocity in the eastern Indian Ocean at 15 days, associated with the propagation of
 487 MRG waves. It should be noted that our estimation relies on 10-day lagrangian mean
 488 velocities : variability at high frequency (time period less than 20 days) is filtered, and
 489 a large part of inertia-gravity and mixed Rossby gravity waves spectrum is missing.

490 A high v-EKE is observed all along the western boundaries of the three basins, from
 491 20°S to 20°N ; interestingly, it is also observed east of topographic obstacles shallower
 492 than 1000m : east of Madagascar Island, of the Mascarene Plateau and of the Chagos-
 493 Laccadive ridge in the Indian Ocean, east of the Gilbert Islands or Marianna trench in
 494 the Pacific Ocean. All these regions, associated with instabilities of deep western bound-
 495 ary currents, or local generation of meridional oscillations by interaction of currents with
 496 topography, are thus potential sources of DEIV radiating away. Meridional EKE is also
 497 higher in the equatorial band in the three basins, particularly in the eastern part of the
 498 Pacific. As discussed in *Ascani et al.* [2010, 2015], this may reflect the presence of ener-
 499 getic waves at depth, excited either by Tropical Instability Waves producing downward

500 propagating MRG wave beams [Weisberg *et al.*, 1979; Boebel *et al.*, 1999; Brandt *et al.*,
501 2006; Bunge *et al.*, 2008; Von Schuckmann *et al.*, 2008] or by wind forcing.

502 Given the previous remarks on the importance of DEIV on the possible impacts
503 on DEC and DTC formations, we understand that its too partial representation in each
504 previously cited study compared to what is observed can be a key factor of misrepresenta-
505 tion of DEC and DTC.

506 5 Perspective and remaining questions

507 5.1 Possible avenues for progress in DEC realism in numerical simula- 508 tions

509 If theoretical framework and idealized simulations are somewhat convincing in their
510 capability to reproduce some pieces of the DEC, realistic simulations are far from ex-
511 hibiting a complete DEC. In a realistic Atlantic equatorial configuration, *Eden and Den-*
512 *gler* [2008] are able to reproduce EDJ with the right characteristics, but with an unde-
513 restimated amplitude compared to observations. Their simulation models the variabi-
514 lity of the western boundary current but does not incorporate the wind forcing. The dif-
515 ficulty of approaching realistic configurations is particularly well illustrated in *Ascani*
516 *et al.* [2015]. In this later study, two solutions are considered : one with a rectangular ba-
517 sin and with a zonally and temporally uniform wind forcing, and one with realistic coast-
518 lines and a zonally varying wind forcing annual cycle. Surprisingly, the first idealized so-
519 lution produces the most realistic deep equatorial circulation. It is not clear whether it
520 is the more realistic wind or the more realistic topography that degrades the realism of
521 the simulation.

522 Several questions thus remain concerning the DEC formation in a realistic frame-
523 work. The first issue is about the capability of models to correctly simulate the DEIV.
524 None of the previous studies did try to combine several sources of variability, even in idea-
525 lized configurations. In the different ocean basins, one can wonder if such a combination
526 of different deep variability sources, with different frequencies, specific zonal or meridio-
527 nal locations, and time-intermittency could improve the simulation of the DEC. More
528 investigations could be done in idealized simulations in combining forcing sources.

529 As suggested in Figures 3, sources of deep variability in meridional velocity can be
530 located along the western boundary, as well as in the center of the basin, especially in
531 the equatorial Pacific Ocean. How different MRG waves, emanating from the western boun-
532 dary current variability and propagating downward from the surface, would merge and
533 produce a coherent DEC is worth investigating. Moreover, the question of destabiliza-
534 tion of a downward propagating wave compared with the destabilization of a primary
535 wave directly forced at depth is not trivial. Another issue concerns the efficiency of a MRG
536 beam energy propagation through a realistic stratification where the thermocline can be
537 a serious obstacle. The representation of DEIV at depth is therefore dependent on a cor-
538 rect behavior of the model regarding its vertical propagation through a variable strati-
539 fication.

540 MRG beams can also be considered as intermittent events forced by strong winds
541 at given times. It would be worth investigating how the DEC may be impacted by time
542 intermittency of the forcing, as it may be by its spatial distribution.

543 Furthermore, equatorial MRG waves can be excited at different frequencies and wa-
544 velengths. In *Hua et al.* [2008]’s theory, short MRG waves are destabilized in a charac-
545 teristic time inversely proportional to their amplitude and wavenumber. Thus, longer waves
546 or weaker waves can remain stable in a basin configuration (see green, orange and cyan
547 points in Figure 4). It is not known how a DEIV full frequency spectrum would behave

548 in a basin configuration. Which frequencies will be destabilized? Which interactions between
549 excited waves will emerge?

550 To the our knowledge, in the Indian Ocean, existing observations did not reveal low-
551 baroclinic zonal jets at low-latitudes. Mean circulation at 1000m inferred from Argo floats
552 drifts do not show coherent zonal features resembling those found in the Atlantic and
553 Pacific Ocean [Cravatte *et al.*, 2014]. The reason for this is not clear. It might arise be-
554 cause the DEIV in the Indian Ocean is too weak, or do not exhibit propitious frequen-
555 cies to be destabilized. Alternatively, it might arise because of distinct mean oceanic ther-
556 mohaline features, or because of a different basin configuration, with oblique coastlines,
557 a northern frontier and a smaller size, inhibiting the development of basin modes for in-
558 stance. Finally, it may be that some jets exist, but at shallower depths, or are masked by
559 much higher variability. This would definitely require specific observations and investi-
560 gations, with idealized model studies. Differences with other basin configurations can be
561 a source of a better understanding of the involved mechanisms in the formation of DTC.

562 **5.2 May Deep Tropical Zonal Circulation (20°N-20°S) be explainable** 563 **with a single theory?**

564 Equatorial idealized studies have currently focused on DEC within 4°N and 4°S.
565 However, as described in section 2, Ollivault *et al.* [2006]; Cravatte *et al.* [2012]; Qiu *et al.*
566 [2013a] and other studies have shown that zonal jets are alternating meridionally over
567 a larger range of latitudes in the Pacific and Atlantic oceans. Could the theories explain-
568 ing DEC be extended to the whole tropical band?

569 A first avenue would be to extend the forcing to higher latitudes. As shown in Fi-
570 gure 3, variability is also found at higher latitudes along the western boundary in re-
571 sponse to large-scale currents fluctuations. A forcing term similar to Gill [1974]’s theory,
572 extending the equatorial response to a DEIV as studied by Hua *et al.* [2008] could be
573 considered.

574 A second avenue would be to evaluate if DTC could be the result of a high meri-
575 dional mode equilibration. We can also wonder if Hua *et al.* [2008]’s theory could pro-
576 duce low-baroclinic Rossby waves with high meridional modes. It would therefore be temp-
577 ting to imagine that the DEC and DTC could be represented as a single structure with
578 an emerging meridional wavelength. The question whether observed Low-Latitude Jets
579 temporality are compatible with a meridional basin mode is still unknown as no obser-
580 vational evidence of a meridional propagation has been provided yet. Another difficulty
581 lies in the complex vertical structure of these jets. They exhibit neither barotropic com-
582 ponent nor a clear baroclinic mode and consist in two systems of jets one on the top of
583 the other (cf. Section 2).

584 Finally, Qiu *et al.* [2013b] proposed a mechanism generating low latitudes zonal jets
585 off equator. Their time-mean solution reproduces a set of such zonal jets, and their ob-
586 servations on two distinct periods encompassing several years suggest that they are at
587 least quasi-stationary features. In their study, the zonal jets meridional scale is fixed by
588 the wind forcing amplitude. The question of how a realistic wind could generate stable
589 meridional scales thus remains open. More generally, the question of the persistence of
590 these jets, their variation or steadiness in latitudinal position and meridional wavelength
591 should be further investigated to see if theories and observations are consistent.

592 **5.3 Is isopycnic turbulence a possible mechanism at low latitudes?**

593 As an alternative to mechanisms involving DEIV and Rossby waves, some authors
594 have argued that the formation of jets in the ocean can be interpreted following Rhines
595 theory [Richards *et al.*, 2006; Baldwin *et al.*, 2007]. Rhines [1975, 1979, 1994] has indeed
596 shown that if the β effect is taken into account, the 2D turbulent cascade to large scales

597 is stopped at some scale where Rossby waves become the driver of the evolution. *Val-*
 598 *lis and Maltrud* [1993] [see also *Theiss*, 2004] have stated that the anisotropy leading to
 599 the emergence of zonal jets come from the fact that the cascade to larger scale can be
 600 pursued much further in the zonal direction, so that turbulence concentrate energy to-
 601 ward large zonal wavelength, eventually leading to the formation of zonal jets¹. This pro-
 602 cess is complemented by the jet sharpening effect discussed in 3.3.2 [see also *Dritschel*
 603 *and McIntyre*, 2008; *Dritschel and Scott*, 2011; *Scott and Dritschel*, 2012, for more de-
 604 tails].

605 In fact, any source of turbulence (from small scale noise to vortical structures gen-
 606 erated by geostrophic instabilities), follows the anisotropic enstrophy cascade and even-
 607 tually leads to the formation of zonal jets [*Baldwin et al.*, 2007; *Kamenkovich et al.*, 2009]).
 608 Since zonal jets alternating with latitude have first been observed in atmospheric flows
 609 of rapidly rotating planets, there exists a very rich literature on this subject in atmos-
 610 pheric and astrophysical sciences (for recent reviews, see for instance *Danilov and Grya-*
 611 *nik* [2004]; *Ingersoll et al.* [2004]; *Liu and Schneider* [2010]; *Jouglu and Dritschel* [2016],
 612 and references therein).

613 *Theiss* [2004] revisited Rhines theory and stated that the formation of zonal jets
 614 is only possible below a critical latitude, beyond which the turbulence remains dominant
 615 and the formation of jets is not possible. Interestingly, this process is consistent with the
 616 potential vorticity structures estimated in the tropical Pacific [*Rowe et al.*, 2000; *Cra-*
 617 *vatte et al.*, 2017; *Delpech et al.*, in prep.]. It is thus also possible to interpret jet-like struc-
 618 tures in the ocean as a consequence of the Rhines theory and PV homogenization by isopycnic
 619 turbulence.

620 However Rhines theory has not been applied to realistic configurations and can-
 621 not explain all observed jet structures, in particular the vertically alternated EDJ, seen
 622 as basin modes, which do not intervene in Rhines theory. In addition, Fig. 3 shows v -
 623 EKE is intensified along western boundaries and the equator (note however that EKE
 624 is here estimated using 10 days averages). In most studies of the Rhines mechanism, isopycnic
 625 turbulence is generated over the whole basin and it is not clear if this is a neces-
 626 sary condition, or if localized turbulence could generate zonal jets extending over the whole
 627 basin.

628 Thus, DEIV direct equilibration and isopycnic turbulence anisotropic rectification
 629 are both mechanisms leading to the formation of zonal jets. Their initial source of energy
 630 differ : equatorial Rossby-Gravity waves for DEIV and small scale turbulence for isopycnic
 631 turbulence. The way energy cascades from large scale forcings is thus crucial to un-
 632 derstand which process dominates. Designing experiments that can help distinguish bet-
 633 tween both processes, maybe differencing the equatorial region and the tropical region,
 634 is also an interesting challenge.

635 6 Conclusion

636 This study reviewed and discussed the current mechanisms explaining the complex
 637 system of zonal jets of the Deep Equatorial and Tropical Circulations. A schematic view
 638 of zonal jets structure as observed in the Pacific and Atlantic oceans is proposed in Fi-
 639 gure 1. Mechanisms proposed in past studies have been summarized and revisited in terms
 640 of a cascade of mechanisms, arising from an initial energy source to the final equilibra-
 641 tion of the Deep Circulation. A schematic view (Figure 2) is developed to classify and
 642 relate them to the different observed zonal jets systems. A particular stress has been put

1. This comes from the fact that Rossby waves having large zonal wavelength evolve very slowly. Turbulent effects are more rapid and thus continue to be the main driver of the evolution in this case, cascading energy to larger scales in the zonal direction.

643 on the importance of the DEIV and its ability to be destabilized into zonal jets. Howe-
644 ver, despite a large amount of theoretical work in the equatorial and tropical region, no
645 consensus to explain the whole circulation has been reached and, above all, no realistic
646 simulation has been able to reproduce convincingly the whole set of zonal jets as obser-
647 ved in the different oceanic basins. Some questions remain open and some new avenues
648 are proposed for further investigations to clarify our global understanding of the Deep
649 Equatorial and Tropical Circulations. We hope that this review will inspire new experi-
650 ments and stimulate new theoretical work related to this exciting research subject.

651 **TABLE 1.** Main abbreviations found in the literature for the different zonal jets or systems of
 652 jets

Abbreviation	Signification
DEC	Deep Equatorial Circulation ^a
DEIV	Deep Equatorial Intraseasonal Variability
EDJ	Equatorial Deep Jets
EEJ	Extra Equatorial Jets
EIC	Equatorial Intermediate Current
SICC	South Intermediate Countercurrent
NICC	North Intermediate Countercurrent
NEIC	North Equatorial Intermediate Current
SEIC	South Equatorial Intermediate Current
LLIC	Low Latitude Intermediate Currents
SCC	Subsurface CounterCurrent
NSCC	North Subsurface CounterCurrent
SSCC	South Subsurface Countercurrent
sSSCC	secondary Southern Subsurface Countercurrent
EUC	Equatorial UnderCurrent
LLSC	Low Latitude Subsurface Countercurrents
SEC	South Equatorial Current
NECC	North Equatorial CounterCurrent
NEC	North Equatorial Current

^aEDJ + EEJ (=EIC) = DEC

	EDJs		
	Atlantic	Indian	Pacific
Latitude range	1°S-1°N		
Longitude extent	Basin-wide		
Depth	500-3000m		
Intensity of zonal velocity	20cm/s	15-20cm/s (in the west)	10cm/s
Characteristic scale	$\Delta z = 500m$	$\Delta z = 300 - 600m$	$\Delta z = 350m$
Permanent or latent character	permanent		
Low frequency temporal variability	4.5 years	4.5 years	12-30 years
	LLSCs		
	Atlantic	Indian	Pacific
Latitude range			10°S-10°N
Longitude extent	N/A	N/A	Full basin : 8000km
Depth	N/A	N/A	Thermocline-600m
Intensity of zonal velocity	N/A	N/A	5 to 20 cm/s, decreasing poleward
Characteristic scale	N/A	N/A	$\Delta y = 3 - 4^\circ$, increasing eastward
Permanent or latent character	N/A	N/A	latent
Low frequency temporal variability	N/A	N/A	N/A
	LLICs		
	Atlantic	Indian	Pacific
Latitude range	12°S-12°N	N/A	16°S-16°N
Longitude extent	Full basin : 2850km	N/A	Full basin : 8000km, with weaker structures at the east.
Depth	800-1000m	N/A	800-1400m
Intensity of zonal velocity	5 to 15 cm/s, decreasing poleward	N/A	5 to 10cm/s, decreasing poleward and eastward
Characteristic scale	$\Delta y = 2 - 3^\circ$	N/A	$\Delta y = 3^\circ$
Permanent or latent character	N/A	N/A	uncertain
Low frequency temporal variability	N/A	N/A	If any, > 10 years

	Wave speeds [ms^{-1}] T [days], L [km], N [s^{-1}], \bar{H} [m], mode m, Fr or M	I	II	III	IV	V (M^*)	destabilization length
Gill [1974]	$c = c_{sR}$	X	X	1	O(1)	$\ll 1$ triads ≥ 1 barotropic instability	
d'Orgeville et al. [2007]	$c = 0.15, c_G = 1.6, c_{sR} = 0.15$ 40, 540, 2.10^{-3} , 5000, 2, $Fr_{Hua} = 0.2$	0.01	0.1	1	1.5	0.7	15°
Hua et al. [2008]	$c = 0.1, c_G = 1.6, c_{sR} = 0.1$ 50, 410, 2.10^{-3} , 5000, 2, $Fr_{Hua} = 0.2$	4.10^{-3}	0.06	1	1	0.8	8°
Fruman et al. [2009]	$c = 0.1, c_G = 3.2, c_{sR} = 0.1$ 50, 400, 2.10^{-3} , 5000, 1, $Fr_{Hua} = 0.15$	1.10^{-3}	0.03	1	1	0.8	10°
Ménesguen et al. [2009a]	$c = 0.1, c_G = 1.6, c_{sR} = 0.1$ 50, 420, 2.10^{-3} , 5000, 2, $Fr_{Hua} = 0.125$	4.10^{-3}	0.06	1	1	0.5	12°
Ascani et al. [2010]	$c = 0.35, c_G = 0.53, c_{sR} = 0.5$ 33, 1000, 2.10^{-3} , 5000, 6, $M_{Asc} = 0.2$	0.3	0.6	1	0.7	0.2	62°
Qiu et al. [2013b]	$c = 0.1, c_G = 3, c_{sR} = 4, c_{lR} = 0.1$ 365, 3000, $g' = 0.018m^2s^{-1}$, 500, X, $U = 0.1ms^{-1}$	2.10^{-5}	1	1	0.03	0.03	11°

TABLE 3. Order of magnitude of the terms (I, II, III, IV, V) present in equation (A.5) for the different models referenced by their associated papers. The parameters of the forcing wave c , the gravity wave speed, the Rossby wave speed (short or long) are also shown. Terms are all compared to the β term in equation (A.5). Nonlinearity (V) is of order O(1) in most of the proposed models which favors barotropic instabilities leading to turbulence and jet formation. In Qiu et al. [2013b], this term is small and linear terms dominate leading to triadic resonance generating eddies which averaged exhibit jets. The length of destabilization is also shown in the last column. Ascani et al. [2010] shows quite a large length due to a faster Yana wave speed, shorter wave number and smaller nonlinearity. Values used here are crude mean estimates used in the models.

654

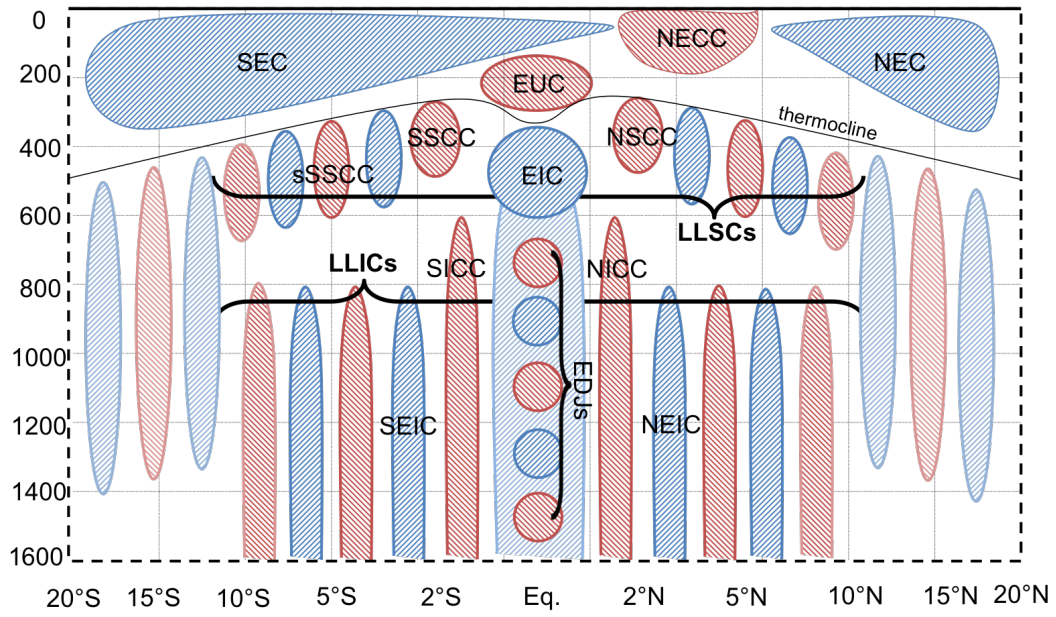
655

656

657

658

659



660 **FIGURE 1.** Schematic representation of the different system of currents found in the tropi-
 661 cal oceans. Dashed blue patterns indicate westward flowing currents and dashed red patterns
 662 indicate eastward flowing currents. The lower boundary of the thermocline is represented with a
 663 solid line. The name of the main currents is indicated (see Table 1). For clarity and readability
 664 reasons, the meridional distance between jets is not scaled.

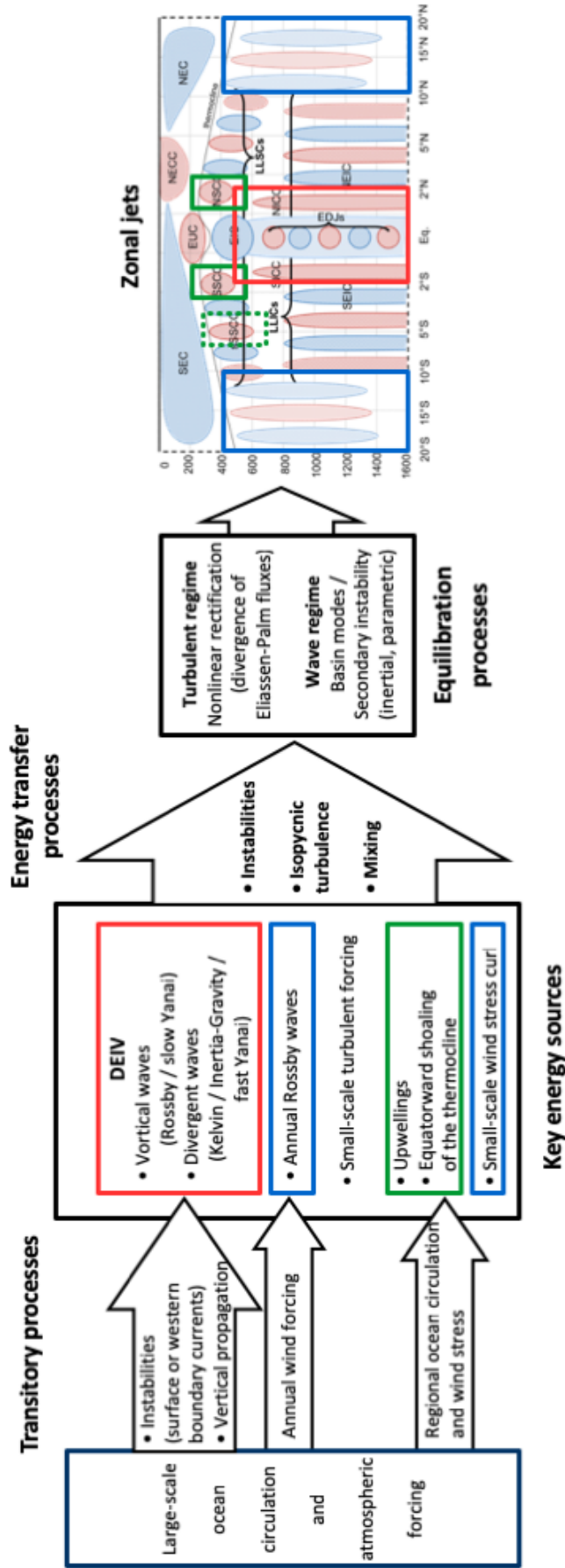


FIGURE 2. Schematic diagram of the cascade leading to the formation of zonal jets in previous studies. Initial large scale forcing excite key intermediate forcings which transfer energy to zonal structure via processes of instability, mixing or isopycnic turbulence. The permanent circulation is the result of equilibration of these zonal structures with oceanic conditions.

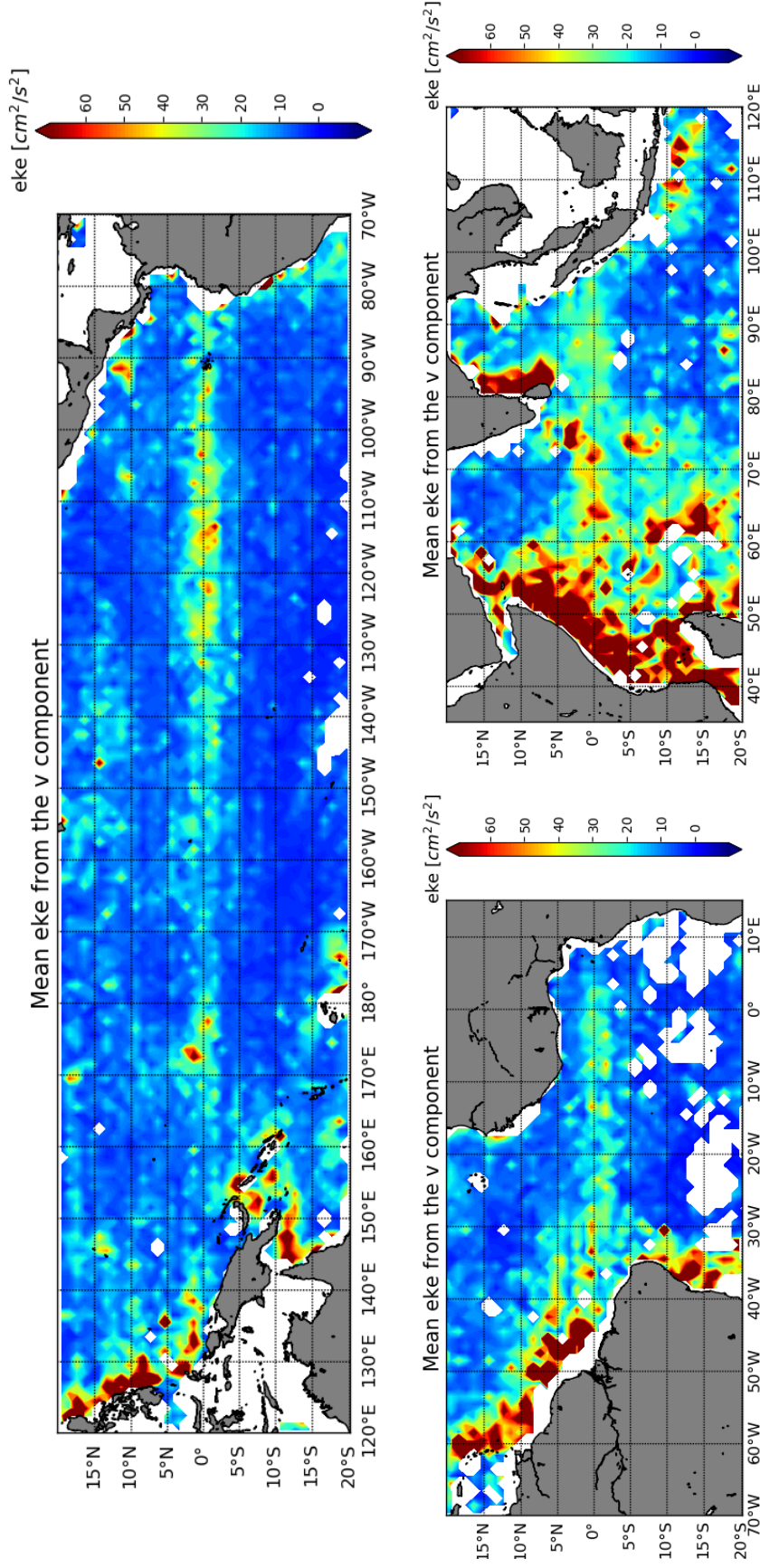
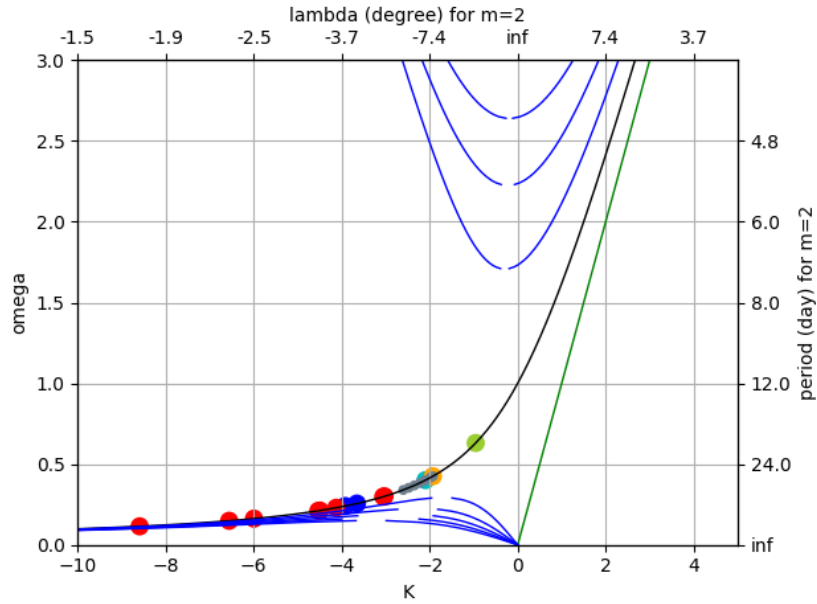


FIGURE 3. Mean Eddy Kinetic Energy of the v component from deep displacement of Argo floats (ANDRO product, *Ollitrault and Colin de Verdière [2014]*). $(v - \bar{v})^2$ where v is the 10-days average meridional velocity of Argo floats displacements at parking depth between 950 and 1050m and \bar{v} the time average 1995-2016 velocity gridded at a resolution $1^\circ \times 1^\circ$.



671 **FIGURE 4.** Different studies discussed in the paper have reproduced a DEC in idealized simu-
 672 lation, prescribing a primary MRG wave. Characteristic values for the primary wave are reported
 673 here in a non-dimensional dispersion diagram. Blue dots are for values found in *Ménesguen et al.*
 674 [2009a], with a cyan dot which is for a case where the primary wave is not unstable within their
 675 50° -long basin. Values corresponding to their barotropic forcing are not represented in this dia-
 676 gram because they lie in the $[-60 -45]$ adimensional k range. *d'Orgeville et al.* [2007]'s values are
 677 in red and orange when the primary wave is stable within their 50° -long basin. The green dot is
 678 a value for the primary wave used in *Ascani et al.* [2010]. Small grey dots stand for an estimation
 679 of the spectrum of primary waves forced in *Ascani et al.* [2015]. This figure illustrates how some
 680 studies consider primary waves that are closed to short Rossby waves characteristics (blue curves
 681 in the low frequency area) and some other depart from these characteristics, approaching a more
 682 divergent dynamics.

683 A: Scaling analysis for equatorial wave dynamics

684 To evaluate the characteristics of the MRG waves used in different studies, we shall
 685 use *Gill* [1974]'s scaling approach, applying it not to the vertical geostrophic vorticity
 686 equation (vortical motions) but to the equatorial vorticity and divergence equation (vor-
 687 tical and divergence motions) governing this region.

688 We consider the vorticity equation

$$\frac{\partial \zeta}{\partial t} + \mathbf{u} \cdot \nabla \zeta + \beta v = -f\delta - \zeta\delta - v_z w_x + u_z w_y \quad (\text{A.1})$$

689 and the divergence equation

$$\frac{\partial \delta}{\partial t} + \mathbf{u} \cdot \nabla \delta + \delta^2 - 2J(u, v) - f\zeta + \beta u = -\nabla^2 \frac{P}{\rho_0} \quad (\text{A.2})$$

690 where $\delta = u_x + v_y = -w_z$ is the horizontal divergence.

691 Combining the x-derivative of the vorticity equation with the x- and t-derivatives
 692 of the divergence equation for the equatorial regions and assuming the pressure field in
 693 hydrostatic balance leads to

$$\underbrace{\delta_{xxt} + f^2 \delta_x + f\beta v_x + \nabla^2 \frac{P_{xt}}{\rho_0}}_{\text{linear}} + \underbrace{f(\mathbf{u} \cdot \nabla \zeta)_x + ONLT}_{\text{non-linear}} = 0 \quad (\text{A.3})$$

694 which non dimensionalized gives

$$\frac{\omega^3}{\omega_G^2 \omega_{sR}} \delta_{xxt} + \frac{\omega}{k\beta L_D^2} \delta_x + v_x + \frac{\omega}{\omega_{sR}} \nabla^2 \frac{P_{xt}}{\rho_0} + M^*[(\mathbf{u} \cdot \nabla \zeta)_x + ONLT] = O(M^{*2}) \quad (\text{A.4})$$

695 where for trapped equatorial waves $K=k$ are zonal wavenumbers, *ONLT* stands
 696 for 'other nonlinear terms' whose form is not important here, and $M^* = \frac{\mathbf{U} \cdot \mathbf{K}}{\omega_{sR}} = \frac{U}{c_{sR}}$.
 697 The term we keep is the advection of vertical vorticity to be able to harmonize and com-
 698 pare the different authors approaches. Wave number k and frequency ω scale as inverse
 699 length and time, U is the zonal velocity magnitude. $\omega_G = \frac{NH}{m\pi} k$ is the Gravity frequency
 700 of mode m , N being the Brunt-Väisälä frequency and H the depth of the ocean. $\omega_{sR} =$
 701 $\frac{\beta}{k}$ is the short Rossby wave frequency. For equatorial trapped waves the deformation ra-
 702 dius is given by $l_D = \sqrt{\frac{c_G}{\beta}}$.

703 In terms of wave phase speeds, dividing frequencies by the zonal wave number, the
 704 above equation becomes :

$$\underbrace{\frac{c^3}{c_G^2 c_{sR}} \delta_{xxt}}_{\text{I}} + \underbrace{\frac{c}{c_G} \delta_x}_{\text{II}} + \underbrace{v_x}_{\text{III}} + \underbrace{\frac{c}{c_{sR}} \nabla^2 \frac{P_{xt}}{\rho_0}}_{\text{IV}} + \underbrace{M^*[(\mathbf{u} \cdot \nabla \zeta)_x + ONLT]}_{\text{V}} = O(M^{*2}) \quad (\text{A.5})$$

705 where $c_G = \frac{NH}{m\pi}$ is the Kelvin wave speed.

706 *Gill* [1974]'s model is obtained by omitting the I and II linear terms

$$v_x + \frac{c}{c_{sR}} \nabla^2 \frac{P_{xt}}{\rho_0} + M^*[(\mathbf{u} \cdot \nabla \zeta)_x] = 0 \quad (\text{A.6})$$

707 For mid-latitude dynamics as in *Qiu et al.* [2013b], the deformation radius is gi-
 708 ven by $\frac{c_G}{f}$ and the term II is scaled as $\frac{c}{\beta L_D^2} = \frac{c}{c_{lR}}$ where c_{lR} is the long Rossby wave
 709 phase speed.

710 To compare the different models, we shall relate the Froude number used by *Hua*
 711 *et al.* [2008] ($Fr_{Hua} = \frac{V}{c_G}$) and the *Ascani et al.* [2015]’s scaling ($M_{Asc} = \frac{U}{c_Y}$) to the
 712 more conventional *Gill* [1974]’s $M^* = \frac{U}{c_{sR}}$, scaling the velocity with the short Rossby
 713 wave speed $c_{sR} = \frac{\beta}{k^2}$.

714 The scaling of the nonlinear term is respectively given by

$$M^* = M_{Asc} \frac{c_Y}{c_{sR}} \quad M^* = Fr_{Hua} \sqrt{\frac{c_G}{c_{sR}}} \frac{c_Y}{c_{sR}} \quad (\text{A.7})$$

715 Since the meridional velocity is used in the Froude number Fr_{Hua} , for consistency,
 716 we have rescaled it to the zonal velocity via the MRG wave (U, V) relation.

717 The ocean models considered here are forced to excite MRG (also called Yanai) waves
 718 $c_Y = c = \frac{\omega}{k}$ while *Qiu et al.* [2013b] forced it with a long Rossby wave $c = \beta L_D^2$ and
 719 *Gill* [1974] with a short Rossby wave $c_{sR} = c = \frac{\omega}{k}$.

720 Acknowledgments

721 We dedicate this review to the memory of Bach Lien Hua, who contributed so much in
 722 the past years to the understanding of the DEC. We thank Bertrand Delorme and Pa-
 723 trice Klein for their help in improving the manuscript. This study has also been possible
 724 thanks to the amount of Argo data, collected and made freely available by the Interna-
 725 tional Argo Program and the national programs that contribute to it (<http://www.argo.ucsd.edu>;
 726 <http://argo.jcommops.org>). The Argo Program is part of the Global Ocean Observing
 727 System (Argo 2000). The authors also thank M. Ollitrault and J.-P. Ranou for making
 728 the ANDRO Atlas available (10.17882/47077).

729 **Références**

- 730 Ascani, F., E. Firing, P. Dutrieux, J. P. McCreary, and A. Ishida (2010), Deep equa-
731 torial ocean circulation induced by a forced-dissipated yanai beam, *Journal of*
732 *Physical Oceanography*, *40*(5), 1118–1142.
- 733 Ascani, F., E. Firing, J. P. McCreary, P. Brandt, and R. J. Greatbatch (2015), The
734 deep equatorial ocean circulation in wind-forced numerical solutions, *Journal of*
735 *Physical Oceanography*, *45*(6), 1709–1734.
- 736 Baldwin, M. P., P. B. Rhines, H.-P. Huang, and M. E. McIntyre (2007), The jet-
737 stream conundrum, *Science*, *315*(5811), 467–468.
- 738 Belmadani, A., N. A. Maximenko, J. P. McCreary, R. Furue, O. V. Melnichenko,
739 N. Schneider, and E. D. Lorenzo (2013), Linear wind-forced beta plumes with
740 application to the hawaiian lee countercurrent, *Journal of Physical Oceanography*,
741 *43*(10), 2071–2094.
- 742 Berloff, P., S. Karabasov, J. T. Farrar, and I. Kamenkovich (2011), On latency of
743 multiple zonal jets in the oceans, *Journal of Fluid Mechanics*, *686*, 534–567.
- 744 Boebel, O., C. Schmid, and W. Zenk (1999), Kinematic elements of antarctic inter-
745 mediate water in the western south atlantic, *Deep Sea Research Part II : Topical*
746 *Studies in Oceanography*, *46*(1-2), 355–392.
- 747 Bourlès, B., C. Andrié, Y. Gouriou, G. Eldin, Y. Du Penhoat, S. Freudenthal,
748 B. Dewitte, F. Gallois, R. Chuchla, F. Baurand, et al. (2003), The deep currents
749 in the eastern equatorial atlantic ocean, *Geophysical research letters*, *30*(5).
- 750 Brandt, P., F. A. Schott, C. Provost, A. Kartavtseff, V. Hormann, B. Bourlès, and
751 J. Fischer (2006), Circulation in the central equatorial atlantic : Mean and intra-
752 seasonal to seasonal variability, *Geophysical Research Letters*, *33*(7).
- 753 Brandt, P., A. Funk, V. Hormann, M. Dengler, R. J. Greatbatch, and J. M. Toole
754 (2011), Interannual atmospheric variability forced by the deep equatorial atlantic
755 ocean, *Nature*, *473*(7348), 497.
- 756 Bunge, L., C. Provost, B. L. Hua, and A. Kartavtseff (2008), Variability at inter-
757 mediate depths at the equator in the atlantic ocean in 2000–06 : Annual cycle,
758 equatorial deep jets, and intraseasonal meridional velocity fluctuations, *Journal of*
759 *Physical Oceanography*, *38*(8), 1794–1806.
- 760 Claus, M., R. J. Greatbatch, P. Brandt, and J. M. Toole (2016), Forcing of the
761 atlantic equatorial deep jets derived from observations, *Journal of Physical Ocea-*
762 *nography*, *46*(12), 3549–3562.
- 763 Cravatte, S., W. S. Kessler, and F. Marin (2012), Intermediate zonal jets in the
764 tropical pacific ocean observed by argo floats, *Journal of Physical Oceanography*,
765 *42*(9), 1475–1485.
- 766 Cravatte, S., F. Marin, and W. S. Kessler (2014), Zonal jets at 1000m in the tro-
767 pics observed from argo floats? drifts, *Mercator Ocean - Quarterly Newsletter*, *50*,
768 11–14.
- 769 Cravatte, S., E. Kestenare, F. Marin, P. Dutrieux, and E. Firing (2017), Subther-
770 mocline and intermediate zonal currents in the tropical pacific ocean : paths and
771 vertical structure, *Journal of Physical Oceanography*, *47*(9), 2305–2324.
- 772 Danilov, S., and V. M. Gryanik (2004), Barotropic beta-plane turbulence in a re-
773 gime with strong zonal jets revisited, *Journal of the atmospheric sciences*, *61*(18),
774 2283–2295.
- 775 Delpech, A., S. Cravatte, F. Marin, and Y. Morel (in prep.), Characterization of
776 deep zonal jets properties in the tropical pacific ocean from high-resolution in-situ
777 data., *In preparation for Journal of Physical Oceanography*.
- 778 Dengler, M., and D. Quadfasel (2002), Equatorial deep jets and abyssal mixing in
779 the indian ocean, *Journal of physical oceanography*, *32*(4), 1165–1180.
- 780 d’Orgeville, M., and B. L. Hua (2005), Equatorial inertial-parametric instability
781 of zonally symmetric oscillating shear flows, *Journal of Fluid Mechanics*, *531*,

- 782 261–291.
- 783 d’Orgeville, M., B. L. Hua, and H. Sasaki (2007), Equatorial deep jets triggered by
784 a large vertical scale variability within the western boundary layer, *Journal of*
785 *marine research*, *65*(1), 1–25.
- 786 Dritschel, D., and M. McIntyre (2008), Multiple jets as pv staircases : the phillips
787 effect and the resilience of eddy-transport barriers, *Journal of the Atmospheric*
788 *Sciences*, *65*(3), 855–874.
- 789 Dritschel, D., and R. Scott (2011), Jet sharpening by turbulent mixing, *Philosophi-*
790 *cal Transactions of the Royal Society of London A : Mathematical, Physical and*
791 *Engineering Sciences*, *369*(1937), 754–770.
- 792 Eden, C., and M. Dengler (2008), Stacked jets in the deep equatorial atlantic ocean,
793 *Journal of Geophysical Research : Oceans*, *113*(C4).
- 794 Eriksen, C. C. (1981), Deep currents and their interpretation as equatorial waves in
795 the western pacific ocean, *Journal of Physical Oceanography*, *11*(1), 48–70.
- 796 Eriksen, C. C. (1982), Geostrophic equatorial deep jets, *J. Mar. Res.*, *40*, 143–157.
- 797 Firing, E. (1987), Deep zonal currents in the central equatorial pacific, *Journal of*
798 *Marine Research*, *45*(4), 791–812.
- 799 Firing, E., S. E. Wijffels, and P. Hacker (1998), Equatorial subthermocline currents
800 across the pacific, *Journal of Geophysical Research : Oceans*, *103*(C10), 21,413–
801 21,423.
- 802 Fruman, M. D., B. L. Hua, and R. Schopp (2009), Equatorial zonal jet formation
803 through the barotropic instability of low-frequency mixed rossby–gravity waves,
804 equilibration by inertial instability, and transition to superrotation, *Journal of the*
805 *Atmospheric Sciences*, *66*(9), 2600–2619.
- 806 Furue, R., J. P. McCreary Jr, Z. Yu, and D. Wang (2007), Dynamics of the southern
807 tsuchiya jet, *Journal of physical oceanography*, *37*(3), 531–553.
- 808 Furue, R., J. P. McCreary Jr, and Z. Yu (2009), Dynamics of the northern tsuchiya
809 jet, *Journal of Physical Oceanography*, *39*(9), 2024–2051.
- 810 Gill, A. (1974), The stability of planetary waves on an infinite beta-plane, *Geophysi-*
811 *cal and Astrophysical Fluid Dynamics*, *6*(1), 29–47.
- 812 Gouriou, Y., B. Bourlès, H. Mercier, and R. Chuchla (1999), Deep jets in the equa-
813 torial atlantic ocean, *Journal of Geophysical Research : Oceans*, *104*(C9), 21,217–
814 21,226.
- 815 Gouriou, Y., C. Andrié, B. Bourlès, S. Freudenthal, S. Arnault, A. Aman, G. El-
816 din, Y. Du Penhoat, F. Baurand, F. Gallois, et al. (2001), Deep circulation in the
817 equatorial atlantic ocean, *Geophysical Research Letters*, *28*(5), 819–822.
- 818 Gouriou, Y., T. Delcroix, and G. Eldin (2006), Upper and intermediate circulation
819 in the western equatorial pacific ocean in october 1999 and april 2000, *Geophysical*
820 *research letters*, *33*(10).
- 821 Hua, B. L., D. W. Moore, and S. Le Gentil (1997), Inertial nonlinear equilibration of
822 equatorial flows, *Journal of Fluid Mechanics*, *331*, 345–371.
- 823 Hua, B. L., F. Marin, and R. Schopp (2003), Three-dimensional dynamics of the
824 subsurface countercurrents and equatorial thermostad. part i : Formulation of
825 the problem and generic properties, *Journal of physical oceanography*, *33*(12),
826 2588–2609.
- 827 Hua, B. L., M. d’Orgeville, M. D. Fruman, C. Ménesguen, R. Schopp, P. Klein, and
828 H. Sasaki (2008), Destabilization of mixed rossby gravity waves and the formation
829 of equatorial zonal jets, *Journal of fluid mechanics*, *610*, 311–341.
- 830 Ingersoll, A. P., T. E. Dowling, P. J. Gierasch, G. S. Orton, P. L. Read, A. Sánchez-
831 Lavega, A. P. Showman, A. A. Simon-Miller, and A. R. Vasavada (2004), Dyna-
832 mics of jupiter’s atmosphere, *Jupiter : The Planet, Satellites and Magnetosphere*,
833 105.
- 834 Ishida, A., H. Mitsudera, Y. Kashino, and T. Kadokura (2005), Equatorial pacific
835 subsurface countercurrents in a high-resolution global ocean circulation model,

- 836 *Journal of Geophysical Research : Oceans*, 110(C7).
- 837 Jochum, M., and P. Malanotte-Rizzoli (2003), The flow of aaiw along the equator, in
838 *Elsevier Oceanography Series*, vol. 68, pp. 193–212, Elsevier.
- 839 Jochum, M., and P. Malanotte-Rizzoli (2004), A new theory for the generation of
840 the equatorial subsurface countercurrents, *Journal of physical oceanography*, 34(4),
841 755–771.
- 842 Johnson, G. C., and D. W. Moore (1997), The pacific subsurface countercurrents
843 and an inertial model, *Journal of Physical Oceanography*, 27(11), 2448–2459.
- 844 Johnson, G. C., and D. Zhang (2003), Structure of the atlantic ocean equatorial
845 deep jets, *Journal of physical oceanography*, 33(3), 600–609.
- 846 Johnson, G. C., B. M. Sloyan, W. S. Kessler, and K. E. McTaggart (2002), Direct
847 measurements of upper ocean currents and water properties across the tropical
848 pacific during the 1990s, *Progress in Oceanography*, 52(1), 31–61.
- 849 Jouglu, T., and D. G. Dritschel (2016), On the origin of jets and vortices in tur-
850 bulent planetary atmospheres., in *EGU General Assembly Conference Abstracts*,
851 vol. 18, p. 803.
- 852 Kamenkovich, I., P. Berloff, and J. Pedlosky (2009), Role of eddy forcing in the dy-
853 namics of multiple zonal jets in a model of the north atlantic, *Journal of Physical*
854 *Oceanography*, 39(6), 1361–1379.
- 855 Kessler, W. S., and L. Gourdeau (2006), Wind-driven zonal jets in the south pacific
856 ocean, *Geophysical Research Letters*, 33(3).
- 857 Leetmaa, A., and P. F. Spain (1981), Results from a velocity transect along the
858 equator from 125 to 159 w, *Journal of Physical Oceanography*, 11(7), 1030–1033.
- 859 Liu, J., and T. Schneider (2010), Mechanisms of jet formation on the giant planets,
860 *Journal of the Atmospheric Sciences*, 67(11), 3652–3672.
- 861 Lorenz, E. N. (1972), Barotropic instability of rossby wave motion, *Journal of the*
862 *Atmospheric Sciences*, 29(2), 258–265.
- 863 Luyten, J. R., and J. Swallow (1976), Equatorial undercurrents, in *Deep Sea Re-*
864 *search and Oceanographic Abstracts*, vol. 23, pp. 999–1001.
- 865 Marin, F., B. L. Hua, and S. Wacongne (2000), The equatorial thermostad and sub-
866 surface countercurrents in the light of the dynamics of atmospheric hadley cells,
867 *Journal of marine research*, 58(3), 405–437.
- 868 Marin, F., R. Schopp, and B. L. Hua (2003), Three-dimensional dynamics of the
869 subsurface countercurrents and equatorial thermostad. part ii : Influence of the
870 large-scale ventilation and of equatorial winds, *Journal of physical oceanography*,
871 33(12), 2610–2626.
- 872 Marin, F., E. Kestenare, T. Delcroix, F. Durand, S. Cravatte, G. Eldin, and
873 R. Bourdalle-Badie (2010), Annual reversal of the equatorial intermediate cur-
874 rent in the pacific : Observations and model diagnostics, *Journal of Physical*
875 *Oceanography*, 40(5), 915–933.
- 876 Matthießen, J.-D., R. J. Greatbatch, P. Brandt, M. Claus, and S.-H. Didwischus
877 (2015), Influence of the equatorial deep jets on the north equatorial countercur-
878 rent, *Ocean Dynamics*, 65(8), 1095–1102.
- 879 Matthießen, J.-D., R. J. Greatbatch, M. Claus, F. Ascani, and P. Brandt (2017),
880 The emergence of equatorial deep jets in an idealised primitive equation model :
881 an interpretation in terms of basin modes, *Ocean Dynamics*, 67(12), 1511–1522.
- 882 McCreary, J., P. Julian, P. Lu, and Z. Yu (2002), Dynamics of the pacific subsurface
883 countercurrents, *Journal of Physical Oceanography*, 32(8), 2379–2404.
- 884 McPhaden, M. J. (1984), On the dynamics of equatorial subsurface countercurrents,
885 *Journal of Physical Oceanography*, 14(7), 1216–1225.
- 886 Ménesguen, C., B. L. Hua, M. D. Fruman, and R. Schopp (2009a), Dynamics of
887 the combined extra-equatorial and equatorial deep jets in the atlantic, *Journal of*
888 *marine research*, 67(3), 323–346.

- 889 Ménesguen, C., B. L. Hua, M. D. Fruman, and R. Schopp (2009b), Intermittent
890 layering in the atlantic equatorial deep jets, *Journal of marine research*, 67(3),
891 347–360.
- 892 Ogata, T., H. Sasaki, V. Murty, M. Sarma, and Y. Masumoto (2008), Intraseasonal
893 meridional current variability in the eastern equatorial indian ocean, *Journal of*
894 *Geophysical Research : Oceans*, 113(C7).
- 895 Ollitrault, M., and A. Colin de Verdière (2014), The ocean general circulation near
896 1000-m depth, *Journal of Physical Oceanography*, 44(1), 384–409.
- 897 Ollitrault, M., and J.-P. Rannou (2013), Andro : An argo-based deep displacement
898 dataset, *Journal of Atmospheric and Oceanic Technology*, 30(4), 759–788.
- 899 Ollitrault, M., M. Lankhorst, D. Fratantoni, P. Richardson, and W. Zenk (2006),
900 Zonal intermediate currents in the equatorial atlantic ocean, *Geophysical research*
901 *letters*, 33(5).
- 902 Ponte, R. M., and J. Luyten (1989), Analysis and interpretation of deep equatorial
903 currents in the central pacific, *Journal of Physical Oceanography*, 19(8), 1025–
904 1038.
- 905 Ponte, R. M., and J. Luyten (1990), Deep velocity measurements in the western
906 equatorial indian ocean, *Journal of physical oceanography*, 20(1), 44–52.
- 907 Qiu, B., D. L. Rudnick, S. Chen, and Y. Kashino (2013a), Quasi-stationary north
908 equatorial undercurrent jets across the tropical north pacific ocean, *Geophysical*
909 *Research Letters*, 40(10), 2183–2187.
- 910 Qiu, B., S. Chen, and H. Sasaki (2013b), Generation of the north equatorial un-
911 dercurrent jets by triad baroclinic rossby wave interactions, *Journal of Physical*
912 *Oceanography*, 43(12), 2682–2698.
- 913 Rhines, P. B. (1975), Waves and turbulence on a beta-plane, *Journal of Fluid Me-*
914 *chanics*, 69(3), 417–443.
- 915 Rhines, P. B. (1979), Geostrophic turbulence, *Annual Review of Fluid Mechanics*,
916 11(1), 401–441.
- 917 Rhines, P. B. (1994), Jets, *Chaos : An Interdisciplinary Journal of Nonlinear*
918 *Science*, 4(2), 313–339.
- 919 Richards, K., N. Maximenko, F. Bryan, and H. Sasaki (2006), Zonal jets in the
920 pacific ocean, *Geophysical research letters*, 33(3).
- 921 Rowe, G. D., E. Firing, and G. C. Johnson (2000), Pacific equatorial subsurface
922 countercurrent velocity, transport, and potential vorticity, *Journal of Physical*
923 *Oceanography*, 30(6), 1172–1187.
- 924 Scott, R. K., and D. G. Dritschel (2012), The structure of zonal jets in geostrophic
925 turbulence, *Journal of Fluid Mechanics*, 711, 576–598.
- 926 Taguchi, B., H. Nakamura, M. Nonaka, N. Komori, A. Kuwano-Yoshida, K. Takaya,
927 and A. Goto (2012), Seasonal evolutions of atmospheric response to decadal sst
928 anomalies in the north pacific subarctic frontal zone : Observations and a coupled
929 model simulation, *Journal of Climate*, 25(1), 111–139.
- 930 Theiss, J. (2004), Equatorward energy cascade, critical latitude, and the pre-
931 dominance of cyclonic vortices in geostrophic turbulence, *Journal of Physical*
932 *Oceanography*, 34(7), 1663–1678, doi :10.1175/1520-0485(2004)034<1663 :EEC-
933 CLA>2.0.CO ;2.
- 934 Vallis, G. K., and M. E. Maltrud (1993), Generation of mean flows and jets on a
935 beta plane and over topography, *Journal of physical oceanography*, 23(7), 1346–
936 1362.
- 937 Von Schuckmann, K., P. Brandt, and C. Eden (2008), Generation of tropical in-
938 stability waves in the atlantic ocean, *Journal of Geophysical Research : Oceans*,
939 113(C8).
- 940 Weisberg, R., A. Horigan, and C. Colin (1979), Equatorially trapped rossby-gravity
941 wave propagation in the gulf of guinea, *Journal of Marine Research*, 37(1).

942 Youngs, M. K., and G. C. Johnson (2015), Basin-wavelength equatorial deep jet
943 signals across three oceans, *Journal of Physical Oceanography*, 45(8), 2134–2148.